

Title	Electroless cobalt deposition from ammonia borane solutions
Authors	Rohan, James F.;Nagle, Lorraine C.;Loughlin, Alan
Publication date	2007-02
Original Citation	Rohan, James F.; Nagle, Lorraine C.; Loughlin, Alan (2007) 'Electroless Cobalt Deposition from Ammonia Borane Solutions'. ECS Transactions, 2 (6):51-59.
Type of publication	Article (peer-reviewed);Conference item
Link to publisher's version	<a href="http://ecst.ecsdl.org/content/2/6/51">http://ecst.ecsdl.org/content/2/6/51</a> - 10.1149/1.2408863
Rights	© 2007 ECS - The Electrochemical Society
Download date	2024-04-26 16:06:28
Item downloaded from	<a href="https://hdl.handle.net/10468/7621">https://hdl.handle.net/10468/7621</a>

# **Electroless cobalt deposition from ammonia borane solutions**

Lorraine C. Nagle, Alan Loughlin and James F. Rohan

Tyndall National Institute, University College Cork, Lee Maltings, Cork, Ireland

Ammonia borane (AB) has been used as a reducing agent in the deposition of cobalt on copper substrates. The bath composition for selective deposition were investigated. The mobile ion free plating bath was pH balanced and buffered using tetramethyl ammonium hydroxide. The codeposition of W with the Co was achieved utilising tungstic acid. The electrochemical analysis of the cobalt deposition and AB oxidation at the operating pH of 9 indicate that the AB oxidation on copper is faster than that on cobalt and that the reaction rate decreases as the deposition proceeds.

## **Introduction**

The multielectron oxidation of amine boranes, in particular dimethylamine borane (DMAB) in aqueous solutions is increasingly being investigated to optimise the low cost electroless deposition of materials for microtechnology applications such as barrier/capping layers for copper IC interconnect (1-10). To this end we have employed microelectrodes to investigate the oxidation mechanism of DMAB in alkaline solutions (11). We recently presented results (12) that showed the simpler amine borane, ammonia borane (AB) may also be utilised as the reducing agent in electroless baths for microelectronics applications. Amine boranes have an advantage over the most widely used alternative reducing agent, hypophosphite, of being catalytically oxidised at copper without the requirement for substrate palladium activation. Dimethylamine borane (DMAB) has been recently employed in the palladium-free electroless deposition of cobalt capping layers on copper for IC interconnect applications (13, 14). In this work we show selective electroless deposition of cobalt from the AB based baths directly on copper without surface activation or the additional step of immersion in a reducing agent solution. The AB based baths are alkali metal free, operate at lower temperatures than DMAB based baths and can deposit at significant rates at lower concentrations.

## **Experimental**

All chemicals used were purchased from Sigma Aldrich and used as received. Deionised water of resistivity 18 M $\Omega$  cm was used to prepare the solutions. The electroless solutions were prepared in glass beakers and the temperature maintained using an Ikamag RCT stirring hotplate with IKATRON ETS-D4 electronic thermometer and IKA H 60 temperature probe. The pH of the solutions was adjusted at room temperature prior to temperature elevation and deposition. The substrates utilised were silicon wafers with 20 nm Ti and 200 nm Cu, patterned with 2.5  $\mu$ m of an alkaline resistant negative photoresist, NT90 supplied by Rohm and Haas (UK). The deposit was analysed using a Hitachi S4000 scanning electron microscope and deposit composition was measured using the attached Avalon energy dispersive x-ray microanalysis probe supplied by PGT. The electrochemical tests were controlled using a CH Instruments potentiostat model 660B. The effective cell volume was 20 ml. All solutions were purged with nitrogen for

20 minutes prior to experiments in order to remove oxygen. All electrochemical experiments were performed at 20 °C. The base Au working electrode was polished on 0.05 µm alumina powder (Struers) before processing. The Pt counter and Ag/AgCl reference electrodes were supplied by IJ Cambria Scientific (UK)

In the case of the copper and cobalt microelectrode analysis the respective metal layer, (Cu or Co) was deposited at a 10 µm Au microelectrode supplied by Princeton Applied Research (suppliers Advanced Measurement Technology, UK). These fabricated microelectrodes were utilised once only. The Cu was deposited on the Au microdisc from a solution of 0.1 mol dm<sup>-3</sup> CuSO<sub>4</sub> by scanning the potential from 0.8 to -0.8 V vs Ag/AgCl at 10 mV s<sup>-1</sup> at 20 °C. The resulting Cu deposit was characterized by recording a cyclic voltammogram in 1 mol dm<sup>-3</sup> NaOH from -1.2 to -0.2 V at 100 mV s<sup>-1</sup>. The monolayer reduction charge associated with Cu(I) to Cu(0) peak seen at -0.58 V vs Ag/AgCl was found to be 2.2×10<sup>-8</sup> C. The deposit was equated to a cylindrical outgrowth from the underlying Au microdisc with a height estimated to be 2.07 ×10<sup>-6</sup> cm and its surface area 7.89×10<sup>-7</sup> cm<sup>2</sup> by comparison with 7.85 × 10<sup>-7</sup> cm<sup>2</sup> for the planar Au microdisc.

Co was also deposited on the Au microdisc for AB oxidation analysis at a Co substrate. The Co was deposited from a solution of 0.083 mol dm<sup>-3</sup> CoSO<sub>4</sub> in 0.25 mol dm<sup>-3</sup> ammonium citrate with TMAH at pH 9 by scanning from 0.6 to -1.2 V vs Ag/AgCl at 100 mV s<sup>-1</sup> at 20 °C. The amount of Co deposited was determined from the charge associated with the Co stripping peak seen at -0.28 V, estimated as 2.4×10<sup>-8</sup> C. The deposit was equated to a cylindrical outgrowth from the underlying Au disc with a height estimated to be 1.05 ×10<sup>-6</sup> cm and surface area 7.87 ×10<sup>-7</sup> cm<sup>2</sup>.

## Results and Discussion

The establishment of a plating solution capable of selectively depositing Co at Cu substrates for potential applications in capping of ULSI copper interconnects may be achieved through the use of borane reducing agents. The AB based bath investigated in this work was formulated to be alkali metal ion free, operating at a pH near 9 for compatibility with organic based dielectrics and capable of operating at lower temperatures than the more common DMAB based baths. Based on previous analysis (12) where Cu deposition was achieved from an AB bath, relatively low concentrations of the metal ion and reducing agent were utilised to give appreciable deposition rates (approximately 2 µm/hr) at moderate temperatures (≤50 °C) in an application area where nanometre thick deposits are required. The deposition rate was found to increase linearly, (from 1.0 to 2.0 µm hr<sup>-1</sup>) with AB concentration over the range 5 to 55 mmol dm<sup>-3</sup>. Higher concentrations of AB led to less stable bath formulations during operation at 50 °C. Using an AB concentration of 0.037 mol dm<sup>-3</sup> and a complexant, ammonium citrate concentration of 0.25 mol dm<sup>-3</sup> the deposition rate was found to increase (from 0.7 to 1.6 µm hr<sup>-1</sup>) over a range of Co ion concentrations from 0.037 to 0.09 mol dm<sup>-3</sup>. Further additions of cobalt above this concentration did not lead to an increase in deposition rate. A concentration of Co utilised in subsequent bath formulations was maintained at 0.083 mol dm<sup>-3</sup>. Stable bath formulations with the above concentrations could be operated over a range of pH values from 8.2 to 10.8 yielding deposition rates of 1.0 to 1.6 µm hr<sup>-1</sup> with an optimal pH of 9 to 9.5. The baths were pH adjusted with tetramethylammonium

hydroxide (TMAH). It can be seen in Figure 1 that 33 nm cobalt may be deposited in 20 minutes at a copper substrate from this bath operating at 30 °C. The deposit thickness increases with temperature up to 50 °C, no further increase in deposition rate was achieved in the range 50 to 60 °C. For 60 minute immersion time typical deposition rates of 1.2 to 1.6  $\mu\text{m hr}^{-1}$  are seen over the temperature range of 37 to 50 °C.

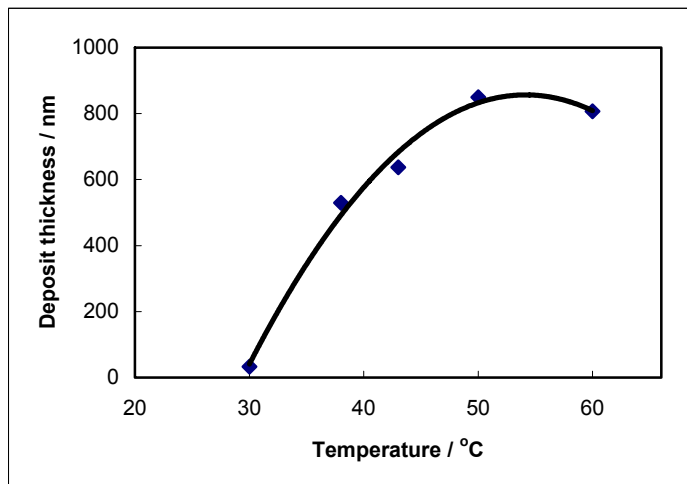


Figure 1. The influence of temperature on the deposition of cobalt at copper from an AB based bath following 20 minute immersion time. Bath composition: ammonium citrate 0.25  $\text{mol dm}^{-3}$ ,  $\text{CoSO}_4 \cdot 7\text{H}_2\text{O}$  0.083  $\text{mol dm}^{-3}$  and AB 0.037  $\text{mol dm}^{-3}$ , pH adjusted with TMAH to 9.

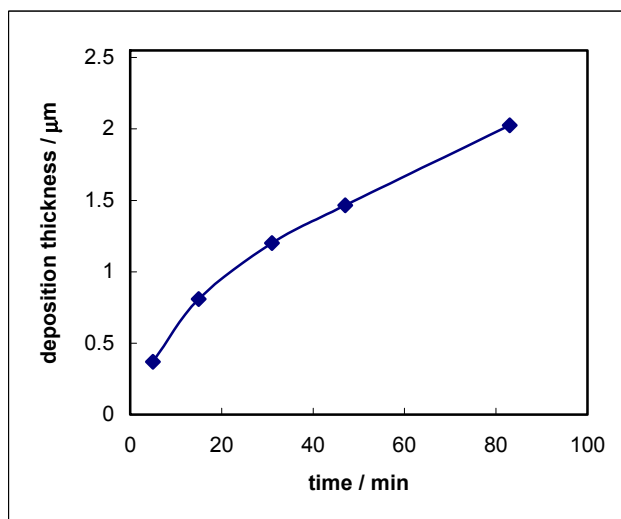
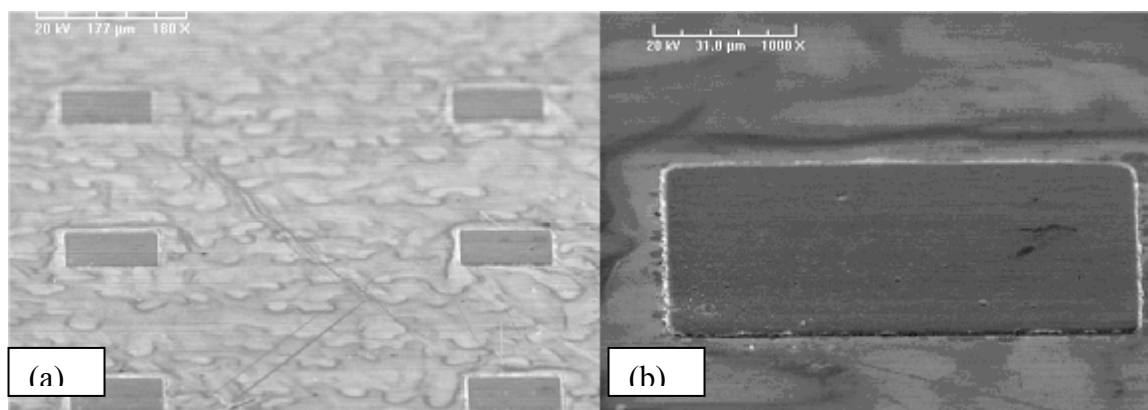


Figure 2. Time dependence of electroless cobalt deposition at copper. Bath composition: ammonium citrate 0.25  $\text{mol dm}^{-3}$ ,  $\text{CoSO}_4 \cdot 7\text{H}_2\text{O}$  0.083  $\text{mol dm}^{-3}$  and AB 0.03  $\text{mol dm}^{-3}$ , at 50 °C and pH adjusted with TMAH to 9.

In Figure 2 the variation of deposit thickness for electroless cobalt deposition at copper substrates with immersion time is shown. It can be seen that the deposition rate decreases with time. As will be discussed below in the electrochemical analysis at microelectrodes

a possible explanation for this behaviour may be that initially the deposit is forming at a copper substrate, which exhibits higher currents for AB oxidation than cobalt which replaces copper as the AB oxidation catalyst as the reaction progresses.

The ability of this bath type to yield selective deposits on copper substrates was demonstrated at a patterned copper wafer (fabrication described in experimental section). The patterned copper pads,  $100 \times 100 \mu\text{m}$ , were exposed to the plating solution at which cobalt deposited. Examples of the selective deposition are shown in Figures 3 (a) and (b). The addition of 120 ppm polyethylene glycol (PEG) and 0.25 ppm thiourea was found to yield smoother deposits with less sidewall growth at the recess in the  $2.5 \mu\text{m}$  thick photoresist.



Figures 3 (a) and (b) SEM images of selective electroless cobalt deposition at a photolithographically patterned copper substrate following resist removal. Bath composition: ammonium citrate  $0.25 \text{ mol dm}^{-3}$ ,  $\text{CoSO}_4 \cdot 7\text{H}_2\text{O}$   $0.083 \text{ mol dm}^{-3}$ , AB  $0.03 \text{ mol dm}^{-3}$ , PEG surfactant 120 ppm and 0.25 ppm thiourea, pH adjusted with TMAH to 9.6 at  $50^\circ\text{C}$ .

In developing effective Co(W,B) barrier layers, it is necessary to incorporate a considerable amount of tungsten, up to 20 at. % (13, 14). We therefore chose to investigate the ability of AB to selectively codeposit W with Co. The data in Table 1 shows the deposit composition for three values of tungstic acid. The boron content in the deposits was below the detection limit of the EDX tool. An example of this selective deposition is shown in Figure 4 for a 10 atomic % W codeposit. In three minutes at  $50^\circ\text{C}$ , 65 nm of a CoW alloy was selectively deposited from the AB based bath. The AB concentration in this bath was  $0.03 \text{ mol dm}^{-3}$ ,  $\text{CoSO}_4 \cdot 7\text{H}_2\text{O}$   $0.083 \text{ mol dm}^{-3}$ , PEG surfactant 120 ppm TMAH at  $50^\circ\text{C}$  and a pH of 9.6.

**Table 1. Influence of tungstic acid concentration in plating bath on W codeposition with Co**

Tungstic acid conc / $\text{mol dm}^{-3}$	At. % Co	At. % W
0.0154	93.61	6.30
0.025	92.97	7.03
0.0382	89.55	10.45

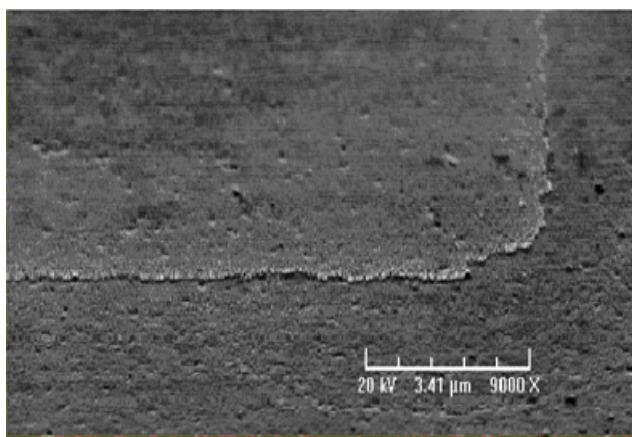


Figure 4. Selective CoW deposit on Cu from an AB based bath. Bath composition: AB  $0.03 \text{ mol dm}^{-3}$ ,  $\text{CoSO}_4 \cdot 7\text{H}_2\text{O}$   $0.083 \text{ mol dm}^{-3}$ , PEG surfactant 120 ppm, pH adjusted with TMAH to 9.6 at  $50^\circ\text{C}$ .

The electrochemical analysis of the Co/AB system was conducted at microelectrodes which have been shown to have a number of advantages in the analysis of electroless plating solution components such as investigation of low concentrations of reducing agent without the additional complication of supporting electrolyte. A copper microelectrode fabricated as described in the experimental section was utilised to examine AB oxidation and cobalt reduction using cyclic voltammetry. It can be seen in Figure 5 that borane oxidation commences on copper at  $-1.01 \text{ V}$  versus Ag/AgCl and the oxidation current reaches a limiting value at  $-0.57 \text{ V}$ .

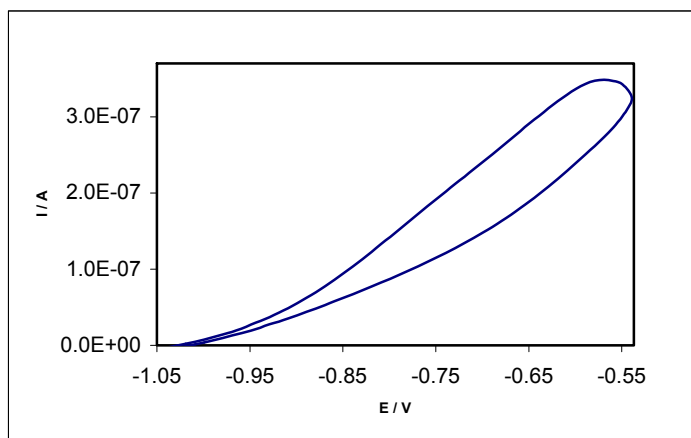


Figure 5. Cyclic voltammogram of copper microdisc recorded in a solution of AB  $0.03 \text{ mol dm}^{-3}$  in  $0.25 \text{ mol dm}^{-3}$  ammonium citrate with TMAH added to adjust pH to 9. The potential was scanned between  $-1.02$  and  $-0.53 \text{ V}$  at  $10 \text{ mV s}^{-1}$ .

It was shown in Figure 6 that in order to deposit cobalt at a gold microdisc it is necessary to negatively scan the potential to below  $-1.0 \text{ V}$ . If the potential was reversed at or before  $-1.0 \text{ V}$  an oxidation peak at  $-0.31 \text{ V}$  indicative of cobalt dissolution was not seen in the reverse positive scan.

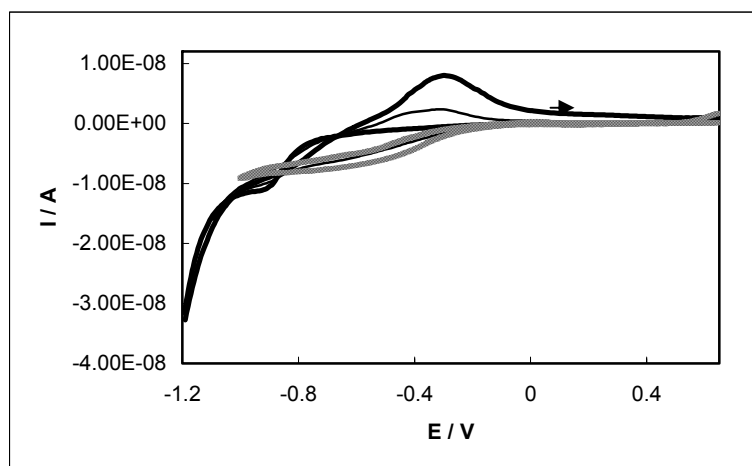


Figure 6. Cyclic voltammogram of gold microdisc recorded in a solution of  $\text{CoSO}_4 \cdot 7\text{H}_2\text{O}$   $0.083 \text{ mol dm}^{-3}$  in  $0.25 \text{ mol dm}^{-3}$  ammonium citrate, pH adjusted with TMAH to 9. The potential was scanned between  $0.65 \text{ V}$  and  $-1.0 \text{ V}$  (.....),  $-1.1 \text{ V}$  (—), and  $-1.2 \text{ V}$  (—) at  $100 \text{ mV s}^{-1}$ .

The deposition and dissolution potentials found here for Co closely agree with those found by both Unwin et. al in a study of the local deposition and dissolution of Co microstructures on Au using SECM (15) and Almeida et al. from an in situ STM study into the morphology of Co clusters on Au(111) (16). The linear sweep voltammogram shown in Figure 7a for cobalt deposition at a copper microelectrode (the preparation of which was described earlier in the experimental section) revealed that cobalt deposition commences at  $-0.95 \text{ V}$ . The resulting Co deposit is stable in this solution until a potential of  $-0.51 \text{ V}$  is reached at which Co dissolution commences with the appearance of an oxidation peak at  $-0.39 \text{ V}$  as shown in Figure 7b. As the potential is further increased above  $-0.27 \text{ V}$  the dissolution of the underlying Cu deposit from the base Au microelectrode commences resulting in the oxidation peak at  $-0.08 \text{ V}$ .

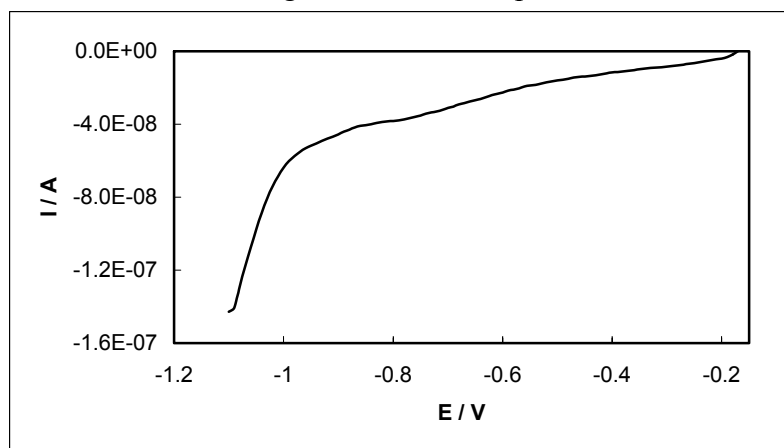


Figure 7a. Linear sweep voltammogram of copper microdisc recorded in a solution of  $\text{CoSO}_4 \cdot 7\text{H}_2\text{O}$   $0.083 \text{ mol dm}^{-3}$  in  $0.25 \text{ mol dm}^{-3}$  ammonium citrate, pH adjusted with TMAH to 9. The potential was scanned from  $-0.18 \text{ V}$  to  $-1.1 \text{ V}$  at  $20 \text{ mV s}^{-1}$ .

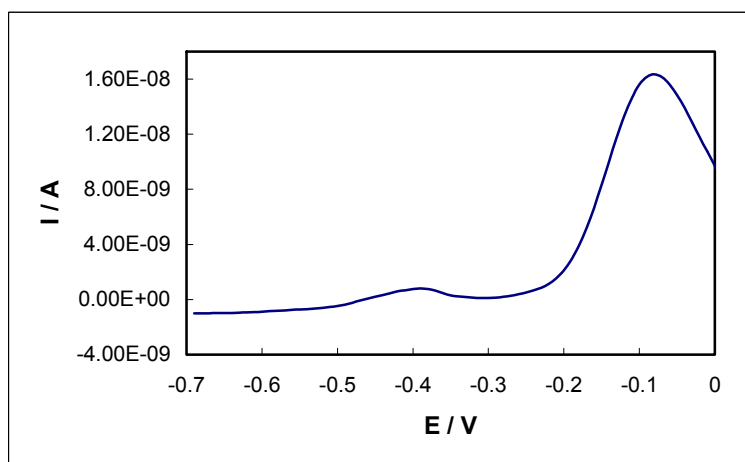


Figure 7b Linear sweep voltammogram of cobalt microdisc in a solution of  $\text{CoSO}_4 \cdot 7\text{H}_2\text{O}$   $0.083 \text{ mol dm}^{-3}$  in  $0.25 \text{ mol dm}^{-3}$  ammonium citrate, pH adjusted with TMAH to 9. The potential was scanned from  $-0.7 \text{ V}$  to  $0.0 \text{ V}$  at  $100 \text{ mV s}^{-1}$ .

A cobalt microelectrode fabricated as described in the experimental section was used to examine AB oxidation. The cyclic voltammogram is shown in Figure 8. It can be seen that borane oxidation commences on cobalt at  $-0.98 \text{ V}$  versus  $\text{Ag}/\text{AgCl}$ . The oxidation current reaches a limiting value at  $-0.54 \text{ V}$ . The oxidation of AB occurs at a somewhat lower rate and at slightly more negative potentials on copper than on cobalt. Similar behaviour was seen for the oxidation response of AB at a copper foil and at a cobalt deposit on copper foil. The onset of borane oxidation commenced at  $-0.92 \text{ V}$  and at  $-0.98 \text{ V}$  on cobalt and copper foil, respectively while the limiting current on copper slightly exceeded that on cobalt.

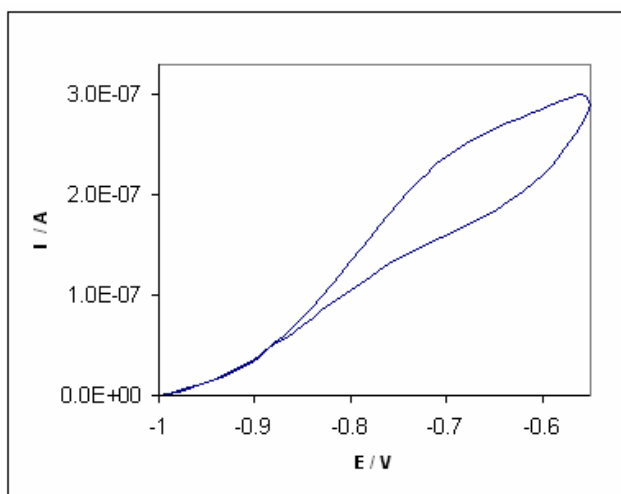


Figure 8. Cyclic voltammogram of Co microdisc recorded in a solution of  $0.03 \text{ mol dm}^{-3}$  AB and  $0.25 \text{ mol dm}^{-3}$  ammonium citrate, pH adjusted with TMAH to 9. The potential was scanned from  $-1.0 \text{ V}$  to  $-0.51 \text{ V}$  at  $100 \text{ mV s}^{-1}$ .

The behaviour of the full cobalt deposition bath at open circuit was analysed at  $33^\circ\text{C}$ . The potential of the copper foil was monitored versus time. The substrate potential decreased from an initial value of  $-0.67 \text{ V}$  to approximately  $-1.0 \text{ V}$  following an



induction period of 200 s. This is consistent with the potential change in the solution as the copper substrate begins to oxidise the borane species in solution leading to the deposition of cobalt on the copper and the gradual shift to less negative potentials as the copper substrate becomes entirely covered with cobalt. The induction period for cobalt deposition may be more closely analysed for precise control of thin film cobalt on copper.

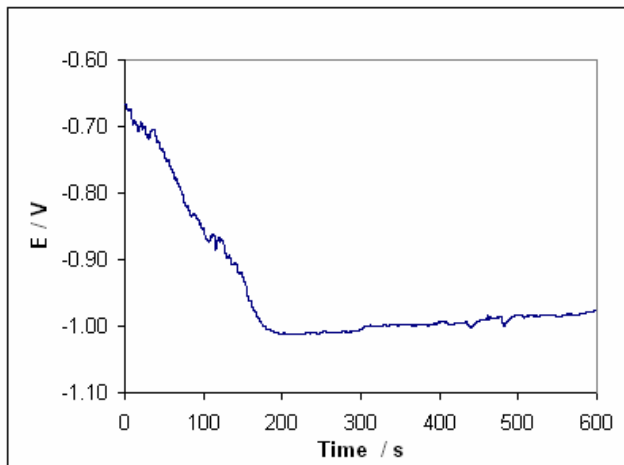


Figure 8. Open circuit potential versus time for electroless Co deposition at Cu foil working electrode versus Ag/AgCl reference electrode in a 2-electrode cell setup. Bath composition:  $\text{CoSO}_4 \cdot 7\text{H}_2\text{O}$   $0.083 \text{ mol dm}^{-3}$ , AB  $0.030 \text{ mol dm}^{-3}$ , ammonium citrate  $0.25 \text{ mol dm}^{-3}$ , pH adjusted with TMAH to 9 at  $33^\circ\text{C}$ .

### Conclusions

Ammonia borane has been utilised for the electroless deposition of cobalt at copper substrates in an alkali metal-free plating solution. This work has demonstrated the ability to selectively deposit cobalt on copper at relatively low temperatures ( $30$  to  $50^\circ\text{C}$ ) at near neutral pH (pH 8-10) for an electroless process, without the need for palladium activation and at an appreciable rate utilising low concentrations of the active materials cobalt and ammonia borane. The codeposition of tungsten has also been achieved at a deposition rate of approximately  $1.8 \mu\text{m/hr}$ . Microelectrode analysis of the half cell reactions indicates that ammonia borane oxidation occurs at a higher rate and at more negative potentials on copper substrates than on cobalt. The corresponding analysis of the full electroless cobalt bath showed an induction period in the low rate deposition at  $33^\circ\text{C}$  prior to a period at the potential of ammonia borane oxidation on copper which was followed by a gradual increase towards the potential where ammonia borane is oxidised on cobalt.

### References

1. F. Pearlstein and R.F. Weightman, *Plat.*, **60**, 474 (1973).
2. M. Lelental, *J. Catal.*, **32**, 429 (1974).
3. C.D. Iacovangelo, *J. Electrochem. Soc.*, **138**, 976 (1991).
4. J.C. Patterson, C. Ni Dheasuna, J. Barrett, T.R. Spalding, M. O'Reilly, X.Jiang and G.M. Crean, *Appl. Surf. Sci.*, **91**, 124 (1995).
5. A. Chiba, H. Haijima and K. Kobayashi, *Surf. Coat. Tech.*, **169-170**, 104 (2003).

6. T. Homma, A. Tamaki, H. Nakai and T. Osaka, *J. Electroanal. Chem.*, **559**, 131 (2003).
7. A. Sargent, O. Sadik and L. Matienzo, *J. Electrochem. Soc.*, **148**, C257 (2001).
8. Y. Yamauchi, T. Yokoshima, H. Mukaibo, M. Tezuka, T. Shigeno, T. Momma, T. Osaka and K. Kuroda, *Chem. Lett.*, **33**, 542 (2004).
9. J.M. Izaki and T. Omi, *J. Electrochem.Soc.*, **144** , L3 (1997).
10. M. Izaki and J.Katayama, *J. Electrochem. Soc.*, **147**, 210 (2000).
11. L.C. Nagle and J.F. Rohan, *Electrochem. Solid-State Lett.*, **8**, C77 (2005)
12. J.F. Rohan, B.M. Ahern and L.C. Nagle, *208th Meeting of The Electrochemical Society. Los Angeles, California October 16-21, 2005; Meet. Abstr. - Electrochem. Soc.* **502**, 691 (2006), DMAB Oxidation for Electroless Deposition from Alkaline Solutions.
13. Y. Sverdlov, V. Bogush, H. Einati and Y. Shacham-Diamand, *J. Electrochem. Soc.*, **152**, (9) C631 (2005).
14. H. Nakaon, T. Itabashi and H. Akahoshi, *J. Electrochem. Soc.*, **152**, (3) C163 (2005).
15. O. de Abril, D. Mandler and P. Unwin, *Electrochem. Solid-State Lett.*, **7** (6) C71 (2004).
16. E.L. Almedia, R.A. Simao, R.F. Selbach, S.L. Diaz and O.R. Mattos, *Acta Microscopica*, **12**(1) 87 (2003).